Evolution of Organo-Cyanometallate Cages: Supramolecular Architectures and New Cs+-Specific Receptors

JULIE L. BOYER, MATTHEW L. KUHLMAN, AND THOMAS B. RAUCHFUSS*

Department of Chemistry, University of Illinois at Urbana-Champaign, Urbana, Illinois 61801

Received August 18, 2006

ABSTRACT

The ability of inorganic cyanometallate polymers to form interesting and useful complexes is well-known. This Account summarizes work, especially in our laboratories, aimed at replicating aspects of this inorganic chemistry in homogeneous solution using organometallic building blocks. A library of molecular organometallic cyanides and Lewis acids, with varying charges and labilities, are shown to give families of neutral and charged cages. Neutral and anionic cages, often molecular boxes, bind larger alkali metals tightly. Cubic frameworks show an unparalleled affinity for cesium cations over potassium cations. Noncubic cages are described including tetrahedranes, defect boxes, trigonal prisms, and hexagonal prisms.

Introduction

There is currently much interest in metal−organic frameworks, that is, multimetallic ensembles that are held

Julie L. Boyer received her B.S. degree in chemistry from University at Buffalo in 2003 and is currently a Ph.D. candidate at UIUC. Her thesis work centers on the synthesis of cyanometallate cages with unique function or architecture.

Matthew L. Kuhlman received his B.S. degree in chemistry from the University of Toledo in 1999 and his Ph.D. in Chemistry from the UIUC in 2004. His thesis work entailed the design of cyanometallate cages for alkali ion separation. He is currently employed as a research scientist at General Electric.
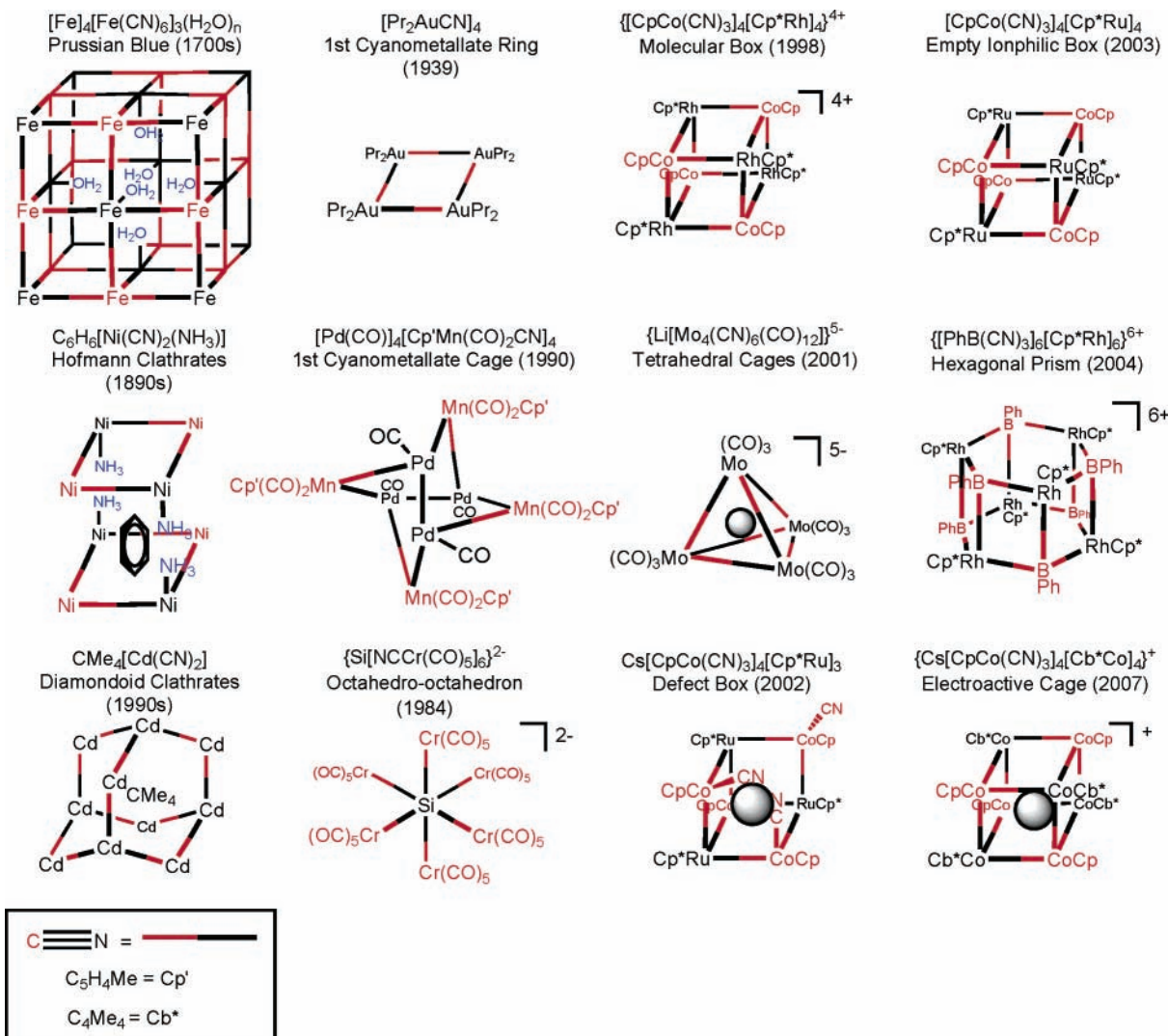
Thomas B. Rauchfuss was born in Baltimore in 1949. He received his Ph.D. from Washington State University in 1975 and after a postdoc at the Australian National University, he joined the faculty at UIUC where he is currently a Professor of Chemistry. In addition to cyanometallates, his research interests include reactions of ligands, synthetic models for hydrogenase enzymes, and metal sulfides.

together through coordination bonds.[1,2] Such hybrid materials have potential as catalysts,[3] molecular sieves,[4] sensors,[5] and in cavity-directed synthesis.[6] Perhaps more importantly, these new materials provide the conceptual foundations for the development of supramolecules that rival those available through organic and bio-organic chemistry.[7,8]

We entered this field through studies on cyanometallates, classical inorganic systems that have a rich history of host-guest behavior. The extensive host-guest behavior of cyanometallates is due in part to their rigid polar framework, which imparts molecular sieving and ion-exchange properties. The host-guest chemistry of polymeric cyanometallates began with the use of the Hofmann clathrates ($[Ni(NH_3)_2][Ni(CN)_4])(C_6H_6)_2$ for the purification of benzene[9] and continues with the application of Prussian Blue (PB, nominally $Fe_7(CN)_{18}\cdot(H_2O)_x$) analogues as sequestrants for Cs^+ and Tl^+.[10] Also relevant are the mineralomimetic cyanometallates wherein M−CN−M groups afford structures resembling silicates in their connectivity.[11] Cyanometallates have shown promise as materials for gas storage and separations.[12] PB analogues have been recently reported as H_2 storage materials.[13] Cobalticyanides reversibly bind O_2, a property applicable to the separation of O_2 from air.[14] These successes, which build upon accelerating advances in microporous coordination solids,[15] raise the prospect for studying analogous behavior in solution using the exquisite analytical and synthetic tools of solution-phase chemistry to explore and elucidate host−guest behavior in molecular cyanometallate cages.

Cyanide frameworks were brought into the molecular regime by the replacement of divergent metal hexa- and tetracyanides with convergent cyanometallate building blocks $L_xM(CN)_y^z$. Examples of cyanometallate rings have long been known starting with $[AuPr_2(CN)]_4$, crystallographically determined in 1939.[16] The size of cyanometallate rings ranges from 9 in $[(CO)_3(NO)W(CN)]_3$ to 24 in a Mn−NC−Fe Schiff base complex.[17] Discrete three-dimensional architectures, however, remained unknown until Braunstein's report of $[(OC)Pd(\mu\text{-}CN)Mn(C_5H_4Me)(CO)_2]_4$, with a still unique structure featuring both bridg-

---

* Author to whom correspondence should be addressed.

Scheme 1. Timeline Illustrating the Progression from Polymeric Molecular Sieves to Organometallic Ionophores[a]

$[Fe]_4[Fe(CN)_6]_3(H_2O)_n$
Prussian Blue (1700s)

$[Pr_2AuCN]_4$
1st Cyanometallate Ring
(1939)

$\{[CpCo(CN)_3]_4[Cp^*Rh]_4\}^{4+}$
Molecular Box (1998)

$[CpCo(CN)_3]_4[Cp^*Ru]_4$
Empty Ionphilic Box (2003)

$C_6H_6[Ni(CN)_2(NH_3)]$
Hofmann Clathrates
(1890s)

$[Pd(CO)]_4[Cp'Mn(CO)_2CN]_4$
1st Cyanometallate Cage (1990)

$\{Li[Mo_4(CN)_6(CO)_{12}]\}^{5-}$
Tetrahedral Cages (2001)

$\{[PhB(CN)_3]_6[Cp^*Rh]_6\}^{6+}$
Hexagonal Prism (2004)

$CMe_4[Cd(CN)_2]$
Diamondoid Clathrates
(1990s)

$\{Si[NCCr(CO)_5]_6\}^{2-}$
Octahedro-octahedron
(1984)

$Cs[CpCo(CN)_3]_4[Cp^*Ru]_3$
Defect Box (2002)

$\{Cs[CpCo(CN)_3]_4[Cb^*Co]_4\}^+$
Electroactive Cage (2007)

$C{\equiv}N =$
$C_5H_4Me = Cp'$
$C_4Me_4 = Cb^*$

[a] The first column indicates major advances in inorganic polymeric cyanide solids, the second column is highlights that portended the area of supramolecular cyanometallate cages, the third and fourth columns indicate landmarks in the work summarized in this Account (the cyanide ligands in $CMe_4Cd(CN)_2$ and $\{Li[Mo_4(CN)_6(CO)_{12}]\}^{5-}$ are disordered).

ing cyanides and metal−metal bonds.[18] Fehlhammer's star clusters represent another class of three-dimensional molecular aggregrates known previous to our work.[19] A 1997 review of cyanometallate ensembles[20] stated that "the construction of cages requires trifunctional building blocks and a lot of luck... One cannot say at the moment how to design the right building blocks for cyanometal cages, but Mother Nature helps sometimes with self-assembly." This Account summarizes our "lucky" experiments on how nature helps with self-assembly (Scheme 1).

I. Cationic Cyanometallate Boxes and Defect Boxes

I.A. Cyanometallate Boxes Form Readily. We began our investigations in 1998 with the synthesis of the molecular box $\{[CpCo(CN)_3]_4[Cp^*Rh]_4\}^{4+}$ (Scheme 2).[21] This species, abbreviated **Co₄Rh₄⁴⁺**, arises from the condensation of equimolar amounts of $[CpCo(CN)_3]^-$ and $[Cp^*Rh-(NCMe)_3]^{2+}$. When the reaction is monitored by ¹H nuclear magnetic resonance (NMR) spectroscopy, several inter-

Scheme 2. Cage-Assembly Reactions for the $[CpCo(CN)_3]^-/[Cp^*Rh]^{2+}$ System
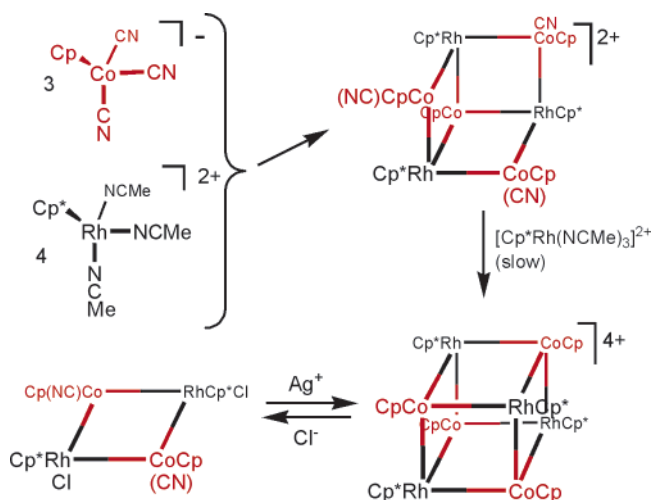
mediates are apparent but after days at room temperature, the exclusive product is the box. Crystallographic analysis

confirmed that eight metal centers are octahedral. IR and ^{13}C NMR spectroscopy demonstrated that the CN linkers are ordered, that is, no Co—C bonds are broken in the condensation. The metal—ligand distances and angles indicate an unstrained species, consistent with the stability of the product. The volume of a cube with 5.1 Å edges is ~132 Å^3; we calculate a van der Waals volume of ~50 Å^3.

The box can also be prepared via a two-step reaction involving the coupling of cyanometallate squares {[CpCo-(μ-CN)$_2$(CN)]$_2$[Cp*RhCl]$_2$} (Scheme 2).[21] The Rh$_2$Co$_2$ square in turn arises via treatment of two equiv of [CpCo(CN)$_3$]$^-$ with [Cp*RhCl$_2$]$_2$, and this method of assembling squares was extended to include {[Cp*Rh(μ-CN)$_2$(CN)]$_2$[(cymene)-RuCl]$_2$} and {[Cp*Rh(μ-CN)$_2$(CN)]$_2$[Cp*RhCl]$_2$}. The box **Co$_4$Rh$_4$$^{4+}$** can be degraded back to the square using excess chloride.

Long has prepared related cyanometallate boxes using metals coordinated by triazacyclononane (TACN).[22] More so than C$_5$R$_5$$^-$, TACN is compatible with paramagnetic metal centers, and thus Long's boxes are promising sources of single molecular magnets. Related magnetic cages have been prepared using tripodal phosphines and trispyrazolylborates.[23] The low charges and diamagnetism of our C$_5$R$_5$$^-$-derived boxes are, however, particularly ideal for the characterization of solution properties.

I.B. Defect Box Cations: {[Cp*Rh(CN)$_3$]$_4$[Cp*Rh]$_3$}$^{2+}$ **and** {[CpCo(CN)$_3$]$_4$[Cp*Rh]$_3$}$^{2+}$. Whereas the condensation of equimolar amounts of [CpCo(CN)$_3$]$^-$ and [Cp*Rh-(NCMe)$_3$]$^{2+}$ affords a box, the corresponding reaction of [CpCo(CN)$_3$]$^-$ with <1 equiv of [Cp*Rh(NCMe)$_3$]$^{2+}$ gives the seven-vertex cage {[CpCo(CN)$_3$]$_4$[Cp*Rh]$_3$}$^{2+}$ (**Co$_4$Rh$_3$$^{2+}$**, Scheme 2). An additional equivalent of [Cp*Rh(NCMe)$_3$]$^{2+}$ converts **Co$_4$Rh$_3$$^{2+}$** into **Co$_4Rh_4$$^{4+}$**, but this reaction is slow, consistent with a pathway that entails substantial disassembly of **Co$_4$Rh$_3$$^{2+}$** followed by reassembly.[24] Obviously, reaction stoichiometry significantly influences the product of cage assembly.

The steric properties of the building blocks can preclude formation of eight-vertex boxes. Thus, condensation of Et$_4$N[Cp*Rh(CN)$_3$] and [Cp*Rh(NCMe)$_3$](PF$_6$)$_2$ exclusively affords {[Cp*Rh(CN)$_3$]$_4$[Cp*Rh]$_3$}$^{2+}$ (**Rh$_7$$^{2+}$**).[25] Molecular models show that close Cp*—Cp* interactions would inhibit the formation of the all-Cp* box {[Cp*Rh-(CN)$_3$]$_4$[Cp*Rh]$_4$}$^{4+}$. The exo orientation of the three terminal cyanides in **Rh$_7$$^{2+}$** generates a closed cavity with the Cp* groups on the terminal Rh subunits forming a "lid" for the cage (Figure 1).

The M$_7$(μ-CN)$_9$ cages are described as "defect boxes" to emphasize their structural relationship to the completed eight-vertex species. As in **Co$_4$Rh$_4$$^{4+}$**, the seven metal centers in **Co$_4$Rh$_3$$^{2+}$** and **Rh$_7$$^{2+}$** are connected by ordered CN ligands. Unlike the M$_8$(CN)$_{12}$ boxes, however, three CN ligands of the defect boxes are terminal (CN$_t$) and the orientation of the terminal cyanides can generate four different isomers (Scheme 3).

I.C. Defect Boxes with Cluster Vertices. Our approach to cyanometallate cages requires electrophiles with three mutually adjacent sites. The potential breadth of this
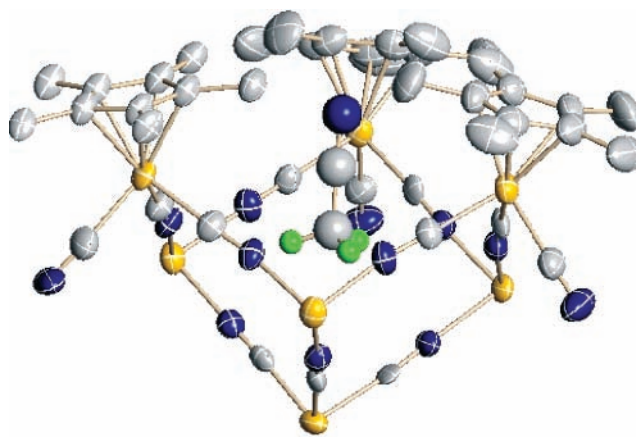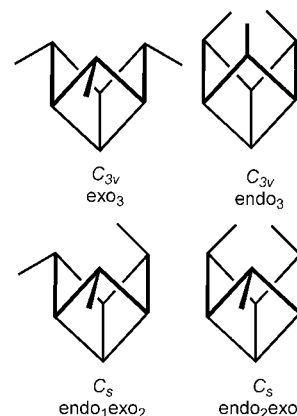

FIGURE 1. Molecular structure of **Rh$_7$$^{2+}$** with an encapsulated acetonitrile guest; the hydrogen atoms are omitted and only the rim Cp* ligands are shown for clarity. Atom coloring scheme: Rh (yellow), N (blue), C (gray).

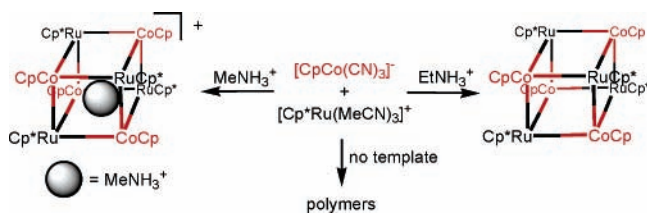**Scheme 3. Possible Isomers of M$_7$(CN)$_{12}$ Defect Boxes**

C_{3v}
exo$_3$

C_{3v}
endo$_3$

C_s
endo$_1$exo$_2$

C_s
endo$_2$exo$_1$

approach is illustrated by the use of a metal cluster bearing a single L$_3$M(NCMe)$_3$^{z} site. In particular, [(cymene)$_2$Ru$_3$S$_2$(NCMe)$_3$]$^{2+}$ was found to efficiently condense with the usual tricyanides [(C$_5$R$_5$)M(CN)$_3$]$^-$. The exclusive products are the defect boxes {[(C$_5$R$_5$)M(CN)$_3$]$_4$-[Ru$_3$S$_2$(cymene)$_2$]$_3$}$^{2+}$ (R = H, M = Co; R = Me, M = Rh).[26] In terms of their M$_7$(μ-CN)$_9$ cores, these M$_{13}$-containing species are quite analogous to **Co$_4$Rh$_3$$^{2+}$** and **Rh$_7$$^{2+}$**.

II. Anionic and Charge-Neutral Cyanometallate Boxes and Defect Boxes

With their considerable internal volumes, cyanometallate boxes should be capable of host–guest chemistry. Although the cationic cyanometallate boxes exhibit no interesting host–guest reactivity, the related neutral and anionic cages proved more fruitful.

II.A. Cyanometallate Boxes with Mo(CO)$_3$ Vertices. Particularly instructive were experiments involving the condensation of sources of "Mo(CO)$_3$". Thus, the 1:1 reaction of Et$_4$N[Cp*Rh(CN)$_3$] and Mo(CO)$_3$(NCMe)$_3$ was expected to generate {[Cp*Rh(μ-CN)$_3$]$_4$[Mo(CO)$_3$]$_4$}$^{4-}$. From such reactions, we were able to obtain only one or two crystals, the structure of which proved to be of (Et$_4$N)$_3$-{K⊂[Cp*Rh(μ-CN)$_3$]$_4$[Mo(CO)$_3$]$_4$}, (Et$_4$N)$_3$[K⊂**Rh$_4$Mo$_4$**], that is, the expected box but containing an encapsulated K$^+$.

Scheme 4. Synthesis of the Ionophilic Cage Co_4Ru_4 and Its Complex $[MeNH_3 \subset Co_4Ru_4]^+$

$MeNH_3^+$ $[CpCo(CN)_3]^-$ $EtNH_3^+$
+
$[Cp*Ru(MeCN)_3]^+$

no template

polymers

$\bigcirc$ = $MeNH_3^+$

Scrutiny of the reagents revealed that our samples of Et_4N-$[Cp*Rh(CN)_3]$ were slightly contaminated with its precursor $K[Cp*Rh(CN)_3]$. Subsequent experiments established that $(Et_4N)_3\{K \subset [Cp*Rh(\mu\text{-}CN)_3]_4[Mo(CO)_3]_4\}$ forms quickly and efficiently when the condensation of $Et_4N[Cp*Rh(CN)_3]$ and $Mo(CO)_3(NCMe)_3$ is conducted in the presence of K^+.[27] An analogous experiment provides the corresponding Cs^+-containing box.

Crystallographic analysis confirmed that the cation is bound within the cubic framework. One striking difference between K^+- and Cs^+-containing cyanometallate boxes is that the Cs^+ is located at the center of the cage whereas the K^+ is disordered over two off-centered sites. The off-center location of K^+ within the cyanometallate box suggests that the $Rh_4Mo_4(CN)_{12}$ cavity might be too large for K^+ and, indeed, ^{133}Cs NMR experiments demonstrate that Cs^+ fully displaces K^+ from the box. A relative binding constant of $K_{Cs}/K_K > 3800$ was determined from competition experiments.

II.B. Cation Binding by $\{[CpCo(CN)_3]_4[Cp*Ru]_4\}$. The affinity of the Rh_4Mo_4 box for alkali metal cations encouraged us to examine charge-neutral boxes, which we expected would be more conveniently soluble than the anionic $Mo-Rh$ cages. This aspect of the work, that is, the variation of the charge properties of the cages, highlights the versatility of the organometallic approach, since many $fac\text{-}[LM(NCMe)_3]^{x+}$ and $fac\text{-}[LM(CN)_3]^{n-}$ building blocks are available. Thus, we began this effort examining the condensation of $[CpCo(CN)_3]^-$ and $[Cp*Ru(NCMe)_3]^+$, completely analogous to the condensation of $[CpCo(CN)_3]^-$ and $[Cp*Rh(NCMe)_3]^{2+}$. We could only obtain consistently soluble cage species when this reaction was conducted in the presence of Cs^+ as a templating cation.[28] Attempted synthesis of a neutral Co_4Ru_4 cage in the absence of alkali metal salts affords insoluble, apparently polymeric products. Subsequent studies showed that in the presence of $EtNH_3^+$, $[CpCo(CN)_3]^-$, and $[Cp*Ru(NCMe)_3]^+$ condense to afford the neutral, empty box $\{[CpCo(CN)_3]_4[Cp*Ru]_4\}$ (Co_4Ru_4). The $EtNH_3^+$ assists in organizing the cyanometallate cage, but it is too large to be contained within it (Scheme 4).[29]

Many ions insert into Co_4Ru_4: Cs^+, K^+, Rb^+, Tl^+, NH_4^+, $MeNH_3^+$, and $N_2H_5^+$ to give the corresponding complexes $\{M \subset [CpCo(CN)_3]_4[Cp*Ru]_4\}^+$, $M \subset Co_4Ru_4^+$. The high affinity of the alkali metals for this cage is attributed to the attractive interactions between the π-bonds of the cyanide ligands with the alkali metal cation.[30] Even cationic boxes form stable complexes with Cs^+, as discussed below. In no case, however, has Na^+ or Li^+ or any di- or trivalent

ion been found to bind; it is apparent that smaller cations ($Na^+ = 4.4$ Å^3, $Li^+ = 1.8$ Å^3) are a poor fit for these ~ 50 Å^3 cages.

Studies on the ammonium-containing box $[NH_4 \subset Co_4$-$Ru_4]^+$ provide insights into the degree to which the box framework shields guest ions from external reagents. Solutions of this species are unreactive toward D_2O, whereas, of course, NH_4^+ and D_2O exchange protons at diffusion-controlled rates. Furthermore, the encapsulated NH_4^+ ($pK_a = 16.46$ in MeCN) is unaffected by strong bases such as quinuclidine ($pK_a = 19.56$ in MeCN). Clearly, confinement within the cage inhibits proton transfer from the stronger acid (NH_4^+) to the base.

II.C. Cation-Binding in Boxes Containing $Cb*Co$ Subunits. The library of neutral cubic frameworks was further extended using the cyclobutadiene-containing building block $[Cb*Co(NCMe)_3]PF_6$ ($Cb* = \eta^4\text{-}Me_4C_4$).[31] The condensation of $[Cb*Co(NCMe)_3]PF_6$ with $KCpCo$-$(CN)_3$ affords $\{K \subset [CpCo(CN)_3]_4[Cb*Co]_4\}PF_6$, $[K \subset Co_8]PF_6$, the only cage of this Account exclusively constructed from first-row transition-metal vertices. The analogous heterometallic cage $\{K \subset [Cp*Rh(CN)_3]_4[Cb*Co]_4\}PF_6$, $[K \subset Rh_4Co_4]$-PF_6, was prepared similarly via the condensation of $K[Cp*Rh(CN)_3]$ and $[Cb*Co(NCMe)_3]PF_6$. As was seen in the other neutral or anionic cages, the K^+ serves as an essential template for cage formation.

The steric properties of $K \subset Co_8^+$, however, differ from previously explored boxes which had contained only octahedral metals with Cp, $Cp*$, or carbonyl coligands. The $Cb*Co^+$ subunit stabilizes larger $N-Co-N$ angles. These slightly obtuse $N-Co-N$ angles destabilize the empty cages: treatment of $PPNCpCo(CN)_3$ and $EtNH_3OTf$ with $[Cb*Co(NCMe)_3]^+$ yields only polymers. The crystallographic analysis of $[K \subset Co_8]PF_6$ showed a rather distorted compressed cube, because of this non-octahedral subunit and the shortening of the $M-NC-M$ distance from the employment of smaller first-row transition-metal vertices. The $M \subset Co_8^+$ cages are more labile than the previous Co_4Ru_4 cage, as demonstrated by the rapid proton exchange between D_2O and $NH_4 \subset Co_8^+$.

II.D. Cs-Centered Defect Boxes $\{M \subset [(C_5R_5)M'(CN)_3]_4$-$[Cp*Ru]_3\}$. The condensation of $[CpCo(CN)_3]^-$ and $[Cp*Ru(NCMe)_3]^+$ in the presence of Cs^+ affords either boxes or defect boxes, depending on the Co/Ru ratio.[28] In this way, we efficiently prepared the violet-colored defect box $\{Cs \subset [CpCo(CN)_3]_4[Cp*Ru]_3\}$, $Cs \subset Co_4Ru_3$. The corresponding condensation of $[Cp*Rh(CN)_3]^-$ and $[Cp*Ru(NCMe)_3]^+$ in the presence of Cs^+ or NH_4^+ proceeds analogously.[32] In this case, the presence of seven bulky $Cp*$ groups precludes the formation of boxes.

In solution, $Cs \subset Co_4Ru_3$ consists of a pair of equilibrating C_s-isomers that differ in stereochemistry of the Cp and CN_t (terminal) ligands on the upper "rim" of the cage (Scheme 3). Each isomer displays a similar ^1H NMR spectrum consisting of singlets with the expected relative intensities of 5:10:5:30:15 (Figure 2). ^{133}Cs NMR spectrum also confirms the presence of two isomers and, using an empirical chemical shift correlation, allows the major
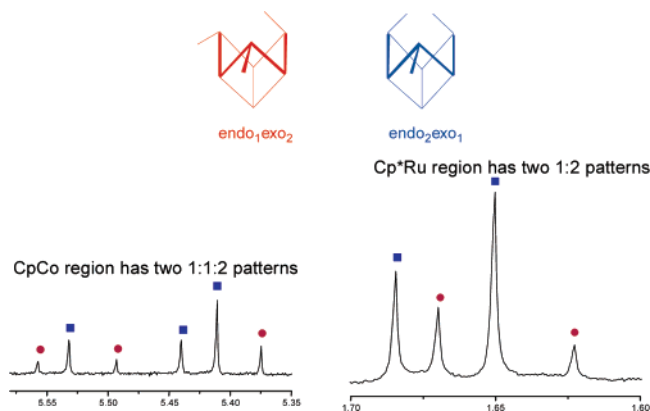
FIGURE 2. ^1H NMR spectrum of $Cs \subset \textbf{Co}_4\textbf{Ru}_3$ in THF solution (red circles = $endo_1exo_2$ isomer; blue squares = $endo_2exo_1$ isomer).

isomer to be assigned as $(exo)_1(endo)_2$ isomer, with two Co*CN* ligands π-bonded to the soft Cs^+ center.[32] Although solutions of $Cs \subset \textbf{Co}_4\textbf{Ru}_3$ feature two isomers, only the $endo_2exo_1$ isomer crystallizes. The crystallographic analysis shows a defect box framework with the average CN_t endo C–Cs and N–Cs distances (3.67 and 3.56 Å) being nearly equal to the average C–Cs and N–Cs distances of the nine Co–*CN*–Ru bridges (3.66 and 3.61 Å). The all-Cp* cages $NH_4 \subset \textbf{Rh}_4\textbf{Ru}_3$ and $Cs \subset \textbf{Rh}_4\textbf{Ru}_3$ only feature the $(exo)_2$-$(endo)_1$ isomer. The Cs–C and Cs–N distances for the terminal endo cyanide in $Cs \subset \textbf{Rh}_4\textbf{Ru}_3$ are 3.40 and 3.25 Å, respectively. For comparison, Cs^+ binds the nine Rh–*CN*–Ru bridges with an average C–Cs distance of 3.67 Å and an average N–Cs distance of 3.59 Å. Thus, the inwardly tilting terminal (endo) cyanide appears to be a strongly bound ligand.

Of all the cages described in this review, $NH_4 \subset \textbf{Rh}_4\textbf{Ru}_3$ is the most distorted. The relatively smaller ionic radius of NH_4^+ ($r_{ionic} = 1.75$ Å vs Cs^+ $r_{ionic} = 1.81$ Å) forces the unique endo CN_t to tilt toward the cage interior, more so than in $Cs \subset \textbf{Rh}_4\textbf{Ru}_3$ (Figure 3). Structural analyses of the three M⊂defect boxes—$Cs \subset \textbf{Co}_4\textbf{Ru}_3$, $NH_4 \subset \textbf{Rh}_4\textbf{Ru}_3$, and $Cs \subset \textbf{Rh}_4\textbf{Ru}_3$—reveal that cage distortion increases as the cationic guest becomes smaller or the *fac*-coligand (Cp vs Cp*) becomes larger.

The IR spectrum of $NH_4 \subset \textbf{Rh}_4\textbf{Ru}_3$ also indicates that NH_4^+ is bound in an unsymmetrical environment, giving rise to three ν_{NH} bands (3196, 3246, and 3270 cm^{-1}). In contrast, the IR spectrum of the box $NH_4 \subset \textbf{Co}_4\textbf{Ru}_4^+$ features a single peak at 3250 cm^{-1}. Only one IR-active mode, T_2, is predicted for NH_4^+ in a totally symmetric environment, reflecting the cubic interior of a $M_8(\mu\text{-CN})_{12}$ box. NMR studies further demonstrate that the NH_4^+ is tumbling rapidly inside of the cage, as only one N*H* signal is observed. Furthermore, it exchanges rapidly with D_2O, whereas $[NH_4 \subset \textbf{Co}_4\textbf{Ru}_4]^+$ is inert toward D_2O.

II.E. {$Cs \subset [CpCo(CN)_3]_4[Cp^*Ru]_3$} as a Tridentate Ligand. The defect box $Cs \subset \textbf{Co}_4\textbf{Ru}_3$ is an excellent tridentate ligand,[28] related to other face-capping ligands such as 1,4,7-triazacyclonane[33] and tris(pyrazolyl)borate.[34] It reacts according to the stoichiometry $Cs \subset \textbf{Co}_4\textbf{Ru}_3 + M^z$ → $[Cs \subset \textbf{Co}_4\textbf{Ru}_3M]^z$, which we call the box completion

process (Scheme 5). Thus, $VCl_3(NCMe)_3$, $[Cp^*Rh(NCMe)_3]^{2+}$, and $[(cymene)_2Ru_2S_2Ru(NCMe)_3]^{2+}$ form the corresponding $[Cs \subset \textbf{Co}_4\textbf{Ru}_3ML_3]^z$ boxes, where $ML_3^z = VCl_3$, $[Cp^*Rh]^{2+}$, and $[(cymene)_2Ru_2S_2Ru]^{2+}$.

The reactivity of $Cs \subset \textbf{Co}_4\textbf{Ru}_3$ toward labile octahedral metal centers can depend on the order of addition. The compound $\{Fe[Cs \subset \textbf{Co}_4\textbf{Ru}_3]_2\}^{2+}$ with idealized D_{3d} symmetry, arises when $[Fe(MeCN)_6]^{2+}$ was added to a solution of $Cs \subset \textbf{Co}_4\textbf{Ru}_3$. In this double box, two $\{Cs \subset [CpCo(CN)_3]_4$-$[Cp^*Ru]_3\}$ cages are conjoined at Fe^{2+} (Scheme 5). The double boxes can be generated from MeCN solvates of Na^+, Co^{2+}, Fe^{2+}, and Ni^{2+}.[28,35] When the order of addition is reversed, one obtains the single boxes $Cs \subset \textbf{Co}_4\textbf{Ru}_3M$-$(NCMe)_3^{2+}$ (M = Fe, Ni).[35] Treatment of $Cs \subset \textbf{Co}_4\textbf{Ru}_3$ with tetrahedral electrophiles ($Cu(NCMe)_4PF_6$ or $AgPF_6$) affords $[Cs \subset \textbf{Co}_4\textbf{Ru}_3M(NCMe)]PF_6$. The MeCN ligands in these Lewis acidic boxes are labile, and thus such cages represent potential catalysts as well as precursors to oligo-cages.

II.F. Insights into Cage Assembly. As mentioned above, addition of 1 equiv of $[Cp^*Rh(NCMe)_3](PF_6)_2$ to $Cs \subset \textbf{Co}_4\textbf{Ru}_3$ efficiently affords the completed box $Cs \subset \textbf{Co}_4\textbf{Ru}_3\textbf{Rh}^{2+}$. In this conversion, the CN_t ligands in $Cs \subset \textbf{Co}_4\textbf{Ru}_3$ must rearrange from exo to endo orientations. The efficiency of this box completion precludes extensive cage fragmentation followed by reassembly.[28] Labeling studies do show, however, that the three $[CpCo(CN)_3]^-$ groups in $Cs \subset \textbf{Co}_4\textbf{Ru}_3$ exchange readily with $[Cp'Co(CN)_3]^-$ ($Cp' = MeC_5H_4$).[35]

It is instructive to contrast the box completion reactions of $Cs \subset \textbf{Co}_4\textbf{Ru}_3 + [Cp^*Ru(NCMe)_3]^+$ with complementary reactions involving $\textbf{Co}_4\textbf{Rh}_3^{2+}$, which lacks a centrally "gluing" Cs^+ center.[36] The $\textbf{Co}_4\textbf{Rh}_3^{2+} + [Cp^*Ru(NCMe)_3]^+$ reaction affords a mixture of $\textbf{Co}_4\textbf{Rh}_4^{4+}$, $\textbf{Co}_4\textbf{Rh}_3\textbf{Ru}^{3+}$, and $\textbf{Co}_4\textbf{Rh}_2\textbf{Ru}_2^{2+}$. These products, especially $\textbf{Co}_4\textbf{Rh}_4^{4+}$, indicate a pathway whereby the starting $\textbf{Co}_4\textbf{Rh}_3^{2+}$ disassembles followed by reformation in a nearly statistical manner. In contrast, $Cs \subset \textbf{Co}_4\textbf{Ru}_3$ appears to remain intact upon complexation to $[Cp^*Rh(NCMe)_3]^{2+}$ to produce $Cs \subset \textbf{Co}_4\textbf{Ru}_3\textbf{Rh}^{2+}$ quantitatively. Slightly different products are obtained when the $\textbf{Co}_4\textbf{Rh}_3^{2+} + [Cp^*Ru(NCMe)_3]^+$ reaction is conducted in the presence of Cs^+. Again, the main products are $\textbf{Co}_4\textbf{Rh}_4^{4+}$ and $\textbf{Co}_4\textbf{Rh}_3\textbf{Ru}^{3+}$, but we also obtained small amounts of $Cs \subset \textbf{Co}_4\textbf{Rh}_2\textbf{Ru}_2^{3+}$ and $Cs \subset \textbf{Co}_4\textbf{Rh}_3\textbf{Ru}^{4+}$. These latter two species are unprecedented examples of Cs^+ bound to cationic receptors.

The preceding box completion reactions were analyzed by assaying the products (by ESI-MS) after the reaction. Using the all-Cp* precursors, we were able to monitor the assembly pathway of $Cs \subset \textbf{Rh}_4\textbf{Ru}_3$ cage in homogeneous solution by ESI-MS (eq 1).[32]

$$3[Cp^*Ru(NCMe)_3]^+ + 4[Cp^*Rh(CN)_3]^- + M^+ \rightarrow$$
$$M \subset [Cp^*Rh(CN)_3]_4[Cp^*Ru]_3$$

$$M \subset \textbf{Rh}_4\textbf{Ru}_3 \quad (M = Cs, NH_4) \qquad (1)$$

The results indicate the intermediacy of $Cs \subset \textbf{Rh}_2\textbf{Ru}_2^+$, which supports the important role for the templating ion in the growth of the cage.
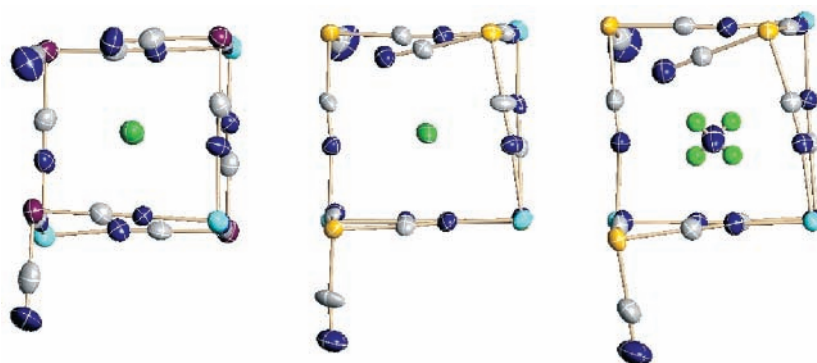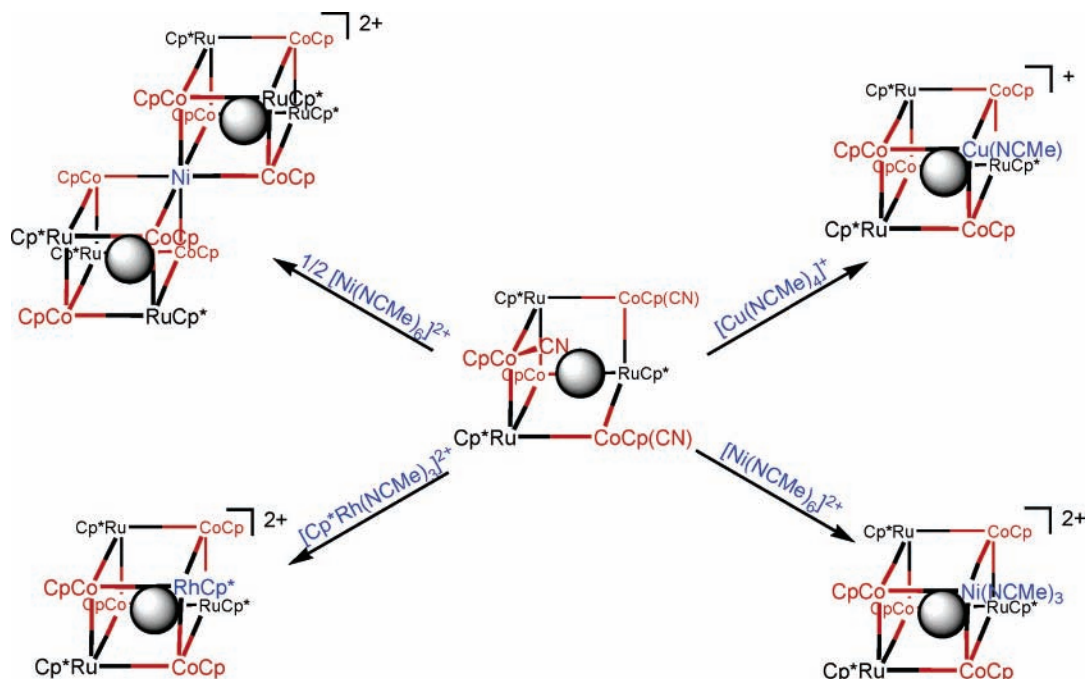
FIGURE 3. The view is approximately parallel to two of the $M_2Ru_2(CN)_4$ faces highlighting the outward or inward bending of the terminal cyanide (M = Co, Rh). Left to right: $Cs\subset Co_4Ru_3$, $Cs\subset Rh_4Ru_3$, $NH_4\subset Rh_4Ru_3$. Atom coloring scheme: Co (purple), Ru (light blue), Rh (yellow), Cs and H (green), C (gray), N (blue).

Scheme 5. Double Boxes, Completed Boxes, and Lewis Acidic Boxes Formed from Metalation of $Cs\subset Co_4Ru_3$ (Gray Sphere = Cs^+)

III. Selective Sequestration of Cs^+ by Cyanometallate Boxes and Defect Boxes

III.A. Ion-Exchange Properties of Cyanometallate Boxes. The availability of the ionophilic box Co_4Ru_4 enabled relatively detailed studies of the ion-binding tendencies of the cages. The kinetic and thermodynamic selectivities are high: when a solution of Co_4Ru_4 is treated with a 1:1 mixture of K^+ and Cs^+, one obtains almost exclusively $K\subset Co_4Ru_4^+$. Over the course of one week, this kinetic species converts to $Cs\subset Co_4Ru_4^+$ (Figure 4). Kinetic studies reveal that the Cs^+-for-K^+ ion exchange process occurs via an initial, rate-determining loss of K^+ followed by the rapid uptake of Cs^+. The rate data allowed us to estimate the binding affinity, K_f, for Cs^+ to be 10^{10}.

III.B. Rh_4Ru_3 Defect Boxes are Kinetically Robust, Rapid, and Highly Selective Complexants for Cs^+. The aforementioned neutral and anionic cages exhibit high affinities for larger monocations, with a marked preference for Cs^+, but the exchange rates for the boxes is slow. We

attribute the sluggishness of this reaction to the inhibiting influence of the Co−CN−Ru connectors that encase the alkali metal ion. These findings guided us to the preparation of ionophilic defect boxes, which retain the high affinity for Cs^+ but have more open structures. The cage $NH_4\subset Rh_4Ru_3$ is ideal for this purpose. In contrast to $NH_4\subset Co_4Ru_4^+$,[29] the ammonium guest in $NH_4\subset Rh_4Ru_3$ is
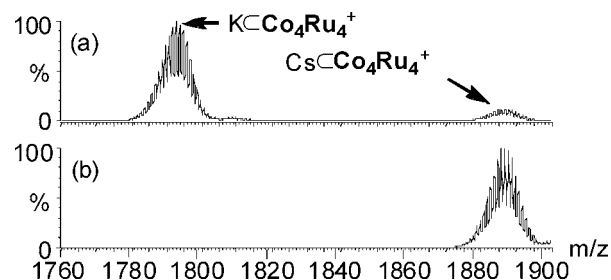

FIGURE 4. ESI-MS for 0.0057 M MeCN solution of Co_4Ru_4 upon treatment with 2 equiv each of K^+ and Cs^+ after 10 min (a) and after 7 days (b).
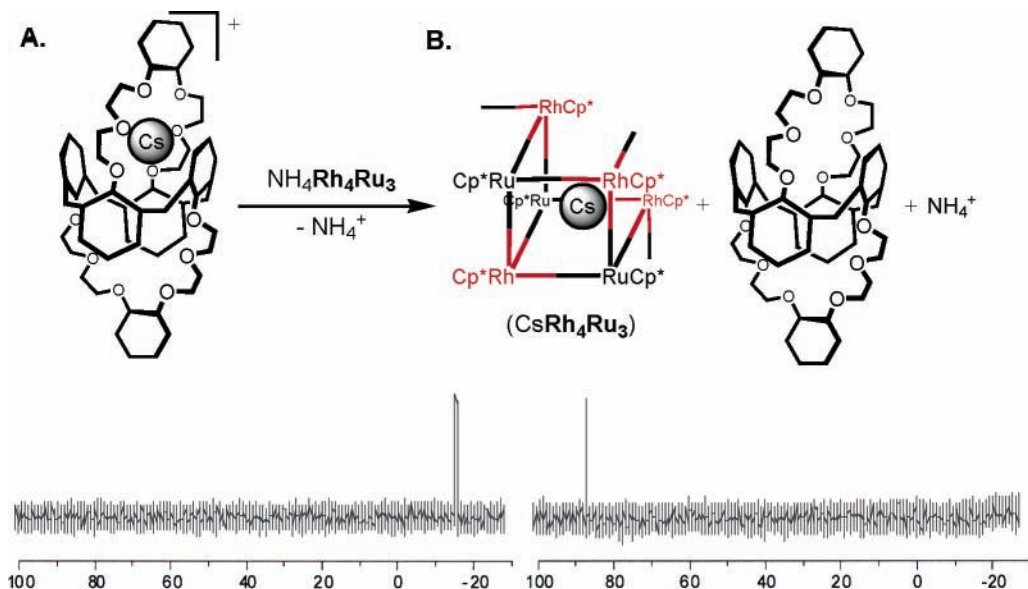
FIGURE 5. 76 MHz ^{133}Cs NMR spectrum of [Cs(BCB6)]$^+$ (MeCN solution) before (A) and after (B) treatment with 1 equiv of NH$_4$⊂**Rh$_4$Ru$_3$** after 30 min. The δ88 signal corresponds to Cs⊂**Rh$_4$Ru$_3$**.
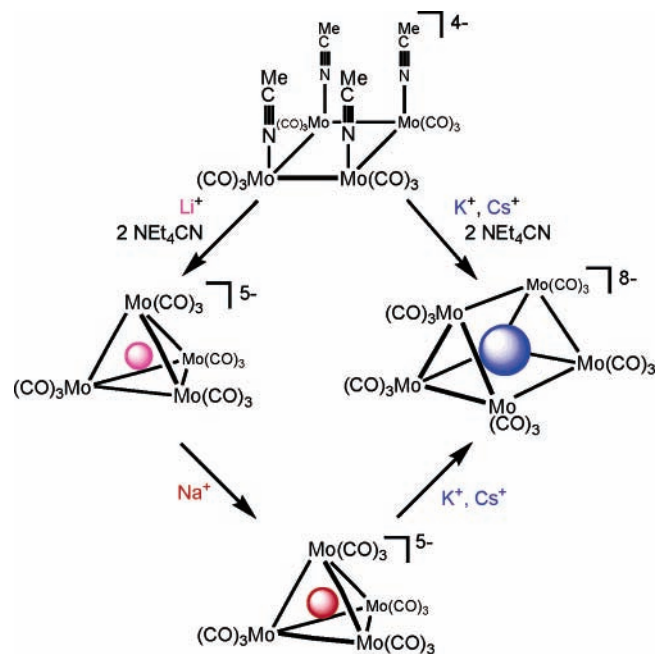
rapidly displaced by Cs$^+$. This result demonstrates the enhanced rate of guest exchange for the defect boxes versus the boxes. The affinity of the host **Rh$_4$Ru$_3$**$^-$, which is never directly observed, for Cs$^+$ was examined in a competition experiment. For the Cs$^+$ source, we used calix[4]arene-bis(benzocrown-6) (BC6B), a high-affinity ($K_{eq} = 10^6$) Cs$^+$-selective ligand.[37] The reaction of a MeCN (or THF) solution of [Cs(BC6B)]$^+$ (^{133}Cs NMR: −δ17) and 1 equiv of NH$_4$⊂**Rh$_4$Ru$_3$** quantitatively converted to Cs⊂**Rh$_4$Ru$_3$** within the time required for NMR analysis, approximately 30 min (Figure 5). The ion exchange of NH$_4$⊂**Rh$_4$Ru$_3$** for Cs$^+$ in presence of 10 equiv K$^+$ yields similar results: an ethereal solution of NH$_4$⊂**Rh$_4$Ru$_3$** extracted Cs$^+$ into an aqueous solution in air.

III.C. Electroactive Cages Containing Cb*Co Are Regeneratable Receptors with Facile Ion Exchange. The lability of the Cb*Co containing cages is demonstrated by the rapid conversion of K⊂**Co$_8$**$^+$ and K⊂**Rh$_4$Co$_4$**$^+$ into the corresponding Cs$^+$-containing cages.[31] The facile ion exchange reflects the lability of the M⊂**Co$_8$**$^+$ framework, as evidenced by vertex-labeling studies. The reaction Cs-Cp′Co(CN)$_3$ + K⊂**Co$_8$**$^+$ results in both alkali ion and vertex exchange {Cs⊂[CpCo(CN)$_3$]$_{4-x}$[Cp′Co(CN)$_3$]$_x$[Cb*Co]$_4$}PF$_6$.

The redox addressable Cb*Co(I) subunits of M⊂**Co$_8$**$^+$ cage enable the tuning of cyanometallate framework's charge. Upon oxidation of the M⊂**Co$_8$**$^+$ with 4 equiv of FcPF$_6$, the encapsulated cation is expelled forming the empty [**Co$_8$**]$^{4+}$ cage. The M⊂**Co$_8$**$^+$ can be regenerated via the reduction of [**Co$_8$**]$^{4+}$ in the presence of alkali metal cations. Reduction in the absence of alkali metal cation generates polymers.

The **Co$_8$** and **Rh$_4$Co$_4$** cages "recognize" the cations in the sense that the encapsulated cations have distinguishable redox properties. The 80 mV difference in half-cell potential between the [K⊂**Co$_8$**]$^+$ and [Cs⊂**Co$_8$**]$^+$ is comparable to the largest effects reported for K$^+$ versus Cs$^+$ response.[38] This effect is slightly obscured by the broad-

Scheme 6. Interconversion of Cyanometallate Cages Composed of Mo(CO)$_3$ Vertices

multielectron nature of the redox wave, and further studies are underway to address this issue.

IV. Noncubic Cyanometallate Cages

IV.A. Assembly with Kinetically Labile Cyanometallates: The Cube Is Not Thermodynamically Favored. Kinetically inert octahedral tricyanometallates force the formation of cages with an even number of vertices on each face, squares and hexagons. When the octahedral tritopic building blocks are kinetically labile, as are the cyanides of Mo(0), the resulting cages are free to adopt a larger variety of structures. An enlightening experiment entailed treatment of Mo(CO)$_3$(NCMe)$_3$ with 1.5 equiv of

FIGURE 6. Molecular structure of the metal cyanide core of the cation in {THF⊂[PhB(CN)$_3$]$_6$[Cp*Rh]$_6$}(OTf)$_6$ with the Cp* and Ph ligands and encapsulated THF omitted for clarity. Atom coloring scheme: Rh (yellow), B (black), N (blue), C (gray).

(Et$_4$N)CN in the presence of alkali metal cations (M$^+$). The resulting cages have the formula M⊂[Mo(CO)$_3$(CN)$_{1.5}$]$_n^{(1-1.5n)}$, where $n = 4$ for tetrahedrane and 6 for a trigonal prism. Cubic cages were not observed. The tetrahedral and trigonal prismatic cages were similarly prepared by the treatment of the square [Mo(CO)$_3$(CN)(NCMe)]$_4$ with 2 equiv CN$^-$ and the templating alkali metal cation (Scheme 6).

These negatively charged cages bind cations at their interiors. The identity of which dictates the structure of the cage.[39,40] Thus, K$^+$ and Cs$^+$ induce the formation of trigonal prismatic cages {M⊂[Mo(CO)$_3$]$_6$(μ-CN)$_9$}$^{8-}$ (Scheme 6). With the smaller Na$^+$ or Li$^+$ as the templating ions, the Mo(CO)$_3$(NCMe)$_3$ + 1.5(Et$_4$N)CN reaction affords the four-vertex tetrahedrane {M⊂[Mo(CO)$_3$]$_4$(μ-CN)$_6$}$^{5-}$. The ^{13}C NMR spectrum of this tetrahedrane features seven CN signals, which demonstrates that the cage exists as a mixture of four isosteric linkage isomers. By monitoring with ^{7}Li and ^{23}Na NMR spectroscopy,[39] we showed that {Li⊂[Mo(CO)$_3$]$_4$(μ-CN)$_6$}$^{5-}$ reacts quantitatively with Na$^+$ to give {Na⊂[Mo(CO)$_3$]$_4$(μ-CN)$_6$}$^{5-}$. Treatment of these tetrahedral cages with K$^+$ and Cs$^+$ gave the trigonal prismatic cages containing the larger cations. Ion exchange of Cs$^+$ into {K⊂[Mo(CO)$_3$]$_6$(μ-CN)$_9$}$^{8-}$ is not observed, suggesting that the trigonal prism strongly incarcerates the K$^+$.

A final illustration of the importance of kinetically well-behaved building blocks is provided by the synthesis of the trigonal prismatic [Cp*$_6$Rh$_6$(CN)$_9$]$^{3+}$.[41] This cage, the framework of which closely resembles that for {M⊂[Mo(CO)$_3$]$_6$(μ-CN)$_9$}$^{8-}$, forms efficiently upon the addition of 1.5 equiv Et$_4$NCN to a solution of [Cp*Rh(NCMe)$_3$]$^{2+}$. The course of this reaction contrasts with the building block approach of [Cp*Rh(CN)$_3$]$^-$ + [Cp*Rh(NCMe)$_3$]$^{2+}$, which efficiently affords the defect box {[Cp*Rh(CN)$_3$]$_4$[Cp*Rh]$_3$}$^{2+}$.

IV.B. Tetrahedral Building Blocks Favor Noncubic Cages. In previous examples, the formation of boxlike cages is a natural consequence of the ∼90° NC−M−CN angles in these precursors, at least for the kinetically robust tricyanides. Efforts to extend the range of structures to new geometries depend on employing non-octahedral cyanometallates where the NC−M−CN angles are >90°. Our attention was drawn to the organoboron tricyanides, such as K[PhB(CN)$_3$]. The recently characterized coordina-

tion solid {Ag[FB(CN)$_3$]}, despite its serendipitous preparation, encouraged us further.[42]

The reaction of [PhB(CN)$_3$]$^-$ and labile sources of "Cp*Rh^{2+}" affords a single product {[PhB(CN)$_3$]$_6$-[Cp*Rh]$_6$}$^{6+}$.[43] X-ray crystallographic analysis established that this species is a 12-vertex hexagonal prism (Figure 6). Two six-membered Rh$_3$B$_3$(CN)$_6$ rings are interconnected by six cyanide ligands to give a cage with idealized D_{3d} symmetry. The edge dimension (B−C−N−Rh) of the hexagonal prism is 4.8 Å yielding a volume of 287 Å^3, whereas the van der Waals' volume of the hexagonal prism is calculated to be 173 Å^3, considerably larger than the ∼50 Å^3 for the molecular boxes.

Summary

Our organometallic approach to cyanometallates powerfully combines the best of both the organometallic and inorganic realms, that is, solubility, control of charge, tunable inertness, and rigidity. The present work has demonstrated certain design rules: favored geometries, the roles of templates, and key building blocks. The scope for expanding this class of compounds is large because many (C$_5$R$_5$)M vertices and analogues are known. Certain cages display very high affinities for alkali metal cations with selectivities that are unachievable with purely organic ligands.

The development of still larger cages as reaction chambers and receptors is an emerging area,[1,7] and we anticipate that the organometallic approach is likely to again be applicable to this challenging but exciting area.

References

(1) (a) Yoshizawa, M.; Fujita, M. Self-Assembled Coordination Cage as a Molecular Flask. *Pure Appl. Chem.* **2005**, *77*, 1107−1112. (b) Fiedler, D.; Leung, D. H.; Bergman, R. G.; Raymond, K. N. Selective Molecular Recognition, C-H Bond Activation, and Catalysis in Nanoscale Reaction Vessels. *Acc. Chem. Res.* **2005**, *38*, 349−358.

(2) (a) Kajitani, H.; Tanabe, Y.; Kuwata, S.; Iwasaki, M.; Ishii, Y. A Cyanamido-Bridged Diiridium Complex: A Reactive Building Block for Polynuclear Cyanamido Complexes. *Organometallics* **2005**, *24*, 2251−2254. (b) Brasey, T.; Scopelliti, R.; Severin, K. Guest-Induced Formation of an Icosahedral Coordination Cage. *Chem. Commun.* **2006**, 3308−3310.

(3) (a) Merlau, M. L.; Del Pilar Mejia, M.; Nguyen, S. T.; Hupp, J. T. Artificial Enzymes Formed Through Directed Assembly of Molecular Square Encapsulated Epoxidation Catalysts. *Angew. Chem., Int. Ed.* **2001**, *40*, 4239−4242. (b) Ito, H.; Kusukawa, T.; Fujita, M. Wacker Oxidation in an Aqueous Phase Through the Reverse Phase-Transfer Catalysis of a Self-Assembled Nanocage. *Chem. Lett.* **2000**, 598−599. (c) Fiedler, D.; Bergman, R. G.; Raymond, K. N. Supramolecular Catalysis of a Unimolecular Transformation: Aza-Cope Rearrangement Within a Self-Assembled Host. *Angew. Chem., Int. Ed.* **2004**, *43*, 6748−6751.

(4) Mueller, A.; Das, S. K.; Talismanov, S.; Roy, S.; Beckmann, E.; Boegge, H.; Schmidtmann, M.; Merca, A.; Berkle, A.; Allouche, L.; Zhou, Y.; Zhang, L. Trapping Cations in Specific Positions in Tuneable "Artificial Cell" Channels: New Nanochemistry Perspectives. *Angew. Chem., Int. Ed.* **2003**, *42*, 5039−5044.

(5) (a) Beer, P. D.; Hayes, E. J. Transition Metal and Organometallic Anion Complexation Agents. *Coord. Chem. Rev.* **2003**, *240*, 167–189. (b) Lehaire, M.-L.; Scopelliti, R.; Piotrowski, H.; Severin, K. Selective Recognition of Fluoride Anion Using a Li$^+$ - Metallacrown Complex. *Angew. Chem., Int. Ed.* **2002**, *41*, 1419–1422.

(6) (a) Yoshizawa, M.; Kusukawa, T.; Fujita, M.; Sakamoto, S.; Yamaguchi, K. Cavity-Directed Synthesis of Labile Silanol Oligomers within Self-Assembled Coordination Cages. *J. Am. Chem. Soc.* **2001**, *123*, 10454–10459. (b) Yoshizawa, M.; Takeyama, Y.; Kusukawa, T.; Fujita, M. Cavity-Directed, Highly Stereoselective [2+2] Photodimerization of Olefins within Self-Assembled Coordination Cages. *Angew. Chem., Int. Ed.* **2002**, *41*, 1347–1349.

(7) Rebek, J., Jr. Simultaneous Encapsulation: Molecules Held at Close Range. *Angew. Chem., Int. Ed.* **2005**, *44*, 2068–2078.

(8) Lehn, J. M. *Supramolecular Chemistry: Concepts and Perspectives*; VCH: Weinhiem, Germany, 1995.

(9) Evans, R. F.; Ormrod, O.; Goalby, B. B.; Staveley, L. A. K. Purification of Benzene. *J. Chem. Soc.* **1950**, 3346.

(10) Prout, W. E.; Russell, E. R.; Groh, H. J. Ion Exchange Absorption of Cesium by Potassium Hexacyanocobaltate Ferrate(II). *J. Inorg. Nucl. Chem.* **1965**, *27*, 473–479.

(11) (a) Iwamoto, T.; Nishikiori, S.; Kitazawa, T.; Yuge, H. Mineralomimetic Chemistry as a Modern Aspect of Co-ordination Chemistry. *J. Chem. Soc., Dalton Trans.* **1997**, 4127–4136. (b) Hoskins, B. F.; Robson, R. Design and Construction of a New Class of Scaffolding-Like Materials Comprising Infinite Polymeric Frameworks of 3D-Linked Molecular Rods. A Reappraisal of the Zinc Cyanide and Cadmium Cyanide Structures and the Synthesis and Structure of the Diamond-Related Frameworks [N(CH$_3$)$_4$][Cu^{I}Zn^{II}-(CN)$_4$] and Cu^I[4,4′,4″,4‴-tetracyanotetraphenylmethane]BF$_4$.xC$_6$H$_5$-NO$_2$. *J. Am. Chem. Soc.* **1990**, *112*, 1546–1554.

(12) Boxhoorn, G.; Moolhuysen, J.; Coolegem, J. G. F.; van Santen, R. A. Cyanometallates: An Underestimated Class of Molecular Sieves. *J. Chem. Soc., Chem. Commun.* **1985**, 1305–1306.

(13) (a) Chapman, K. W.; Southon, P. D.; Weeks, C. L.; Kepert, C. J. Reversible Hydrogen Gas Uptake in Nanoporous Prussian Blue Analogues. *Chem. Commun.* **2005**, 3322–3324. (b) Kaye, S. S.; Long, J. R. Hydrogen Storage in the Dehydrated Prussian Blue Analogues M$_3$[Co(CN)$_6$]$_2$ (M = Mn, Fe, Co, Ni, Cu, Zn). *J. Am. Chem. Soc.* **2005**, *127*, 6506–6507.

(14) (a) Ramprasad, D.; Markley, T. J.; Pez, G. P. Solid State Cyanocobaltates that Reversibly Bind Dioxygen: Synthesis, Structure and Reactivity Relationships. *J. Mol. Catal. A* **1997**, *117*, 273–278. (b) Meier, I. K.; Pearlstein, R. M.; Ramprasad, D.; Pez, G. P. Tetrabutylammonium Tetracyanocobaltate(II) Dioxygen Carriers. *Inorg. Chem.* **1997**, *36*, 1707–1714. (c) Ramprasad, D.; Pez, G. P.; Toby, B. H.; Markley, T. J.; Pearlstein, R. M. Solid State Lithium Cyanocobaltates with a High Capacity for Reversible Dioxygen Binding: Synthesis, Reactivity, and Structures. *J. Am. Chem. Soc.* **1995**, *117*, 10694–10701.

(15) (a) Rosi, N. L.; Eckert, J.; Eddaoudi, M.; Vodak, D. T.; Kim, J.; O'Keeffe, M.; Yaghi, O. M. Hydrogen Storage in Microporous Metal-Organic Frameworks. *Science* **2003**, *300*, 1127–1130. (b) Sudik, A. C.; Millward, A. R.; Ockwig, N. W.; Cote, A. P.; Kim, J.; Yaghi, O. M. Design, Synthesis, Structure, and Gas (N$_2$, Ar, CO$_2$, CH$_4$, and H$_2$) Sorption Properties of Porous Metal-Organic Tetrahedral and Heterocuboidal Polyhedra. *J. Am. Chem. Soc.* **2005**, *127*, 7110–7118.

(16) Phillips, R. F.; Powell, H. M. The Crystal Structure of Di-n-propylmonocyanidegold. *Proc. R. Soc.* **1939**, *173*, 147–159.

(17) (a) Schinnerling, P.; Thewalt, U. Die Struktur [Cp$_2$Ti(III)(CN)]$_4$. *J. Organomet. Chem.* **1992**, *431*, 41–45. (b) Davies, J. A.; Hartley, F. R.; Murray, S. G.; Pierce-Butler, M. A. X-ray Crystal Structure of a Unique Cyano-Bridged Cyclic Palladium(II) Trimer. *J. Chem. Soc., Dalton Trans.* **1983**, 1305–1308. (c) Dawes, H. M.; Hursthouse, M. B.; del Paggio, A. A.; Muetterties, E. L.; Parkins, A. W. The Preparation and X-ray Crystal Structure of W$_3$(μ-CN)$_3$(NO)$_3$-(CO)$_9$. *Polyhedron* **1985**, *4*, 379–382. (d) Evans, W. J.; Drummond, D. K. Reactivity of Isocyanides with (C$_5$Me$_5$)$_2$Sm(THF)$_2$: Synthesis and Structure of Trimeric [(C$_5$Me$_5$)$_2$Sm(CNC$_6$H$_{11}$)(μ-CN)]$_3$. *Organometallics* **1988**, *7*, 797–802. (e) Darensbourg, D. J.; Lee, W.-Z.; Adams, M. J.; Larkins, D. L.; Reibenspies, J. H. Diamond-Shaped Heterometallic Complexes of Iron(II) and Copper(I) Bridged by Cyanide Ligands. *Inorg. Chem.* **1999**, *38*, 1378–1379. (f) Obora, Y.; Ohta, T.; Stern, C. L.; Marks, T. J. Organolanthanide-Catalyzed Imine Hydrogenation. Scope, Selectivity, Mechanistic Observations, and Unusual Byproducts. *J. Am. Chem. Soc.* **1997**, *119*, 3745–3755. (g) Lai, S.-W.; Cheung, K.-K.; Chan, M. C.-W.; Che, C.-M. [{Pt(CN)(C$_{10}$H$_{21}$N$_4$)}$_6$]: A Luminescent Hexanuclear Platinum(II) Macrocycle Containing Chelating Dicarbene and Bridging Cyanide Ligands. *Angew. Chem., Int. Ed.* **1998**, *37*, 182–184. (h)

Ni, Z.-H.; Kou, H.-Z.; Zhang, L.-F.; Ge, C.; Cui, A.-L.; Wang, R.-J.; Li, Y.; Sato, O. [Mn^{III}(salen)]$_6$[Fe^{III}(bpmb)(CN)$_2$]$_6$.7H$_2$O: A Cyanide-Bridged Nanosized Molecular Wheel. *Angew. Chem., Int. Ed.* **2005**, *44*, 7742–7745.

(18) Braunstein, P.; Oswald, B.; Tiripicchio, A.; Camellini, M. T. Novel Binding Mode for a Cyanometalate Ligand: Synthesis and Crystal Structure of the Mn$_4$Pd$_4$ Cluster [(OC)Pd(μ-CN)Mn(η-C$_5$H$_4$Me)-(CO)$_2$]$_4$ Containing an Orthogonal Arrangement of Helical Units. *Angew. Chem., Int. Ed. Engl.* **1990**, *29*, 1140–1143.

(19) (a) Fritz, M.; Rieger, D.; Baer, E.; Beck, G.; Fuchs, J.; Holzmann, G.; Fehlhammer, W. P. Octahedro Octahedra and Tetrahedra. II. Tetra- to Heptanuclear Carbonyl(cyano)Chromato, -Molybdato and -Tungstato Complexes of 3d Metals. *Inorg. Chim. Acta* **1992**, *198–200*, 513–526. (b) Baer, E.; Fehlhammer, W. P.; Breitinger, D. K.; Mink, J. Organometallic Octahedro-octahedra: Hexakis-{pentacarbonyl(cyano)chromato-N}silicate, -germanate, and -stannate. *Inorg. Chim. Acta* **1984**, *82*, L17–L19.

(20) Vahrenkamp, H.; Geiss, A.; Richardson, G. N. Cyanide-Bridged Oligonuclear Complexes: Features and Attractions. *J. Chem. Soc., Dalton Trans.* **1997**, 3643–3651.

(21) Klausmeyer, K. K.; Rauchfuss, T. B.; Wilson, S. R. Stepwise Assembly of [(C$_5$H$_5$)$_4$(C$_5$Me$_5$)$_4$Co$_4$Rh$_4$(CN)$_{12}$]$^{4+}$, an "Organometallic Box". *Angew. Chem., Int. Ed.* **1998**, *37*, 1694–1696.

(22) Heinrich, J. L.; Berseth, P. A.; Long, J. R. Molecular Prussian Blue Analogues: Synthesis and Structure of Cubic Cr$_4$Co$_4$(CN)$_{12}$ and Co$_8$(CN)$_{12}$ Clusters. *Chem. Commun.* **1998**, 1231–1232.

(23) (a) Schelter, E. J.; Prosvirin, A. V.; Reiff, W. M.; Dunbar, K. R. Unusual Magnetic Metal-Cyanide Cubes of Re^{II} with Alternating Octahedral and Tetrahedral Corners. *Angew. Chem., Int. Ed.* **2004**, *43*, 4912–4915. (b) Li, D.; Parkin, S.; Wang, G.; Yee, G. T.; Clérac, R.; Wernsdorfer, W.; Holmes, S. M. An S = 6 Cyanide-Bridged Octanuclear Fe^{III}$_4$Ni^{II}$_4$ Complex that Exhibits Slow Relaxation of the Magnetization. *J. Am. Chem. Soc.* **2006**, *128*, 4214–4215.

(24) Contakes, S. M. Synthesis and Characterization of Organometallic Cyanides and Phthalocyanines. Ph.D. Thesis, University of Illinois-UC, Urbana, IL, 2001.

(25) Contakes, S. M.; Klausmeyer, K. K.; Milberg, R. M.; Wilson, S. R.; Rauchfuss, T. B. The Seven-Component Assembly of the Bowl-Shaped Cages Cp*$_7$Rh$_7$(CN)$_{12}$$^{2+}$ and Cp*$_7$Rh$_3$Ir$_4$(CN)$_{12}$$^{2+}$. *Organometallics* **1998**, *17*, 3633–3635.

(26) Kuhlman, M. L.; Rauchfuss, T. B. Hybrid Cluster-Cages Formed via Cyanometalate Condensation: CsCo$_4$Ru$_6$S$_2$(CN)$_{12}$, Co$_4$-Ru$_9$S$_6$(CN)$_9$, and Rh$_4$Ru$_9$S$_6$(CN)$_9$ Frameworks. *Inorg. Chem.* **2004**, *43*, 430–435.

(27) Klausmeyer, K. K.; Wilson, S. R.; Rauchfuss, T. B. Alkali Metal-Templated Assembly of Cyanometallate Boxes (NEt$_4$)$_3${M[Cp*Rh-(CN)$_3$]$_4$[Mo(CO)$_3$]$_4$} (M = K, Cs): Selective Binding of Cs$^+$. *J. Am. Chem. Soc.* **1999**, *121*, 2705–2711.

(28) Contakes, S. M.; Kuhlman, M. L.; Ramesh, M.; Wilson, S. R.; Rauchfuss, T. B. Systematic Assembly of the Double Molecular Boxes: {Cs[CpCo(CN)$_3$]$_4$[Cp*Ru]$_3$} as a Tridentate Ligand. *Proc. Natl. Acad. Sci.* **2002**, *99*, 4889–4893.

(29) Hsu, S. C. N.; Ramesh, M.; Espenson, J. H.; Rauchfuss, T. B. Membership Rules for a Molecular Box: The Admission Process and Protection Provided to Guest Molecules. *Angew. Chem., Int. Ed.* **2003**, *42*, 2663–2666.

(30) (a) Bryan, J. C.; Kavallieratos, K.; Sachleben, R. A. Unusual Ligand Coordination for Cesium. *Inorg. Chem.* **2000**, *39*, 1568–1572. (b) Kopp, M. R.; Neumueller, B. The Reaction of Cyanide Ions with Trimethylgallium. The Crystal Structures of [Cs{CN(GaMe$_3$)}]$_n$ and [Cs(toluene)$_2${CN(GaMe$_3$)$_2$}]$_n$. *Z. Anorg. Allg. Chem.* **1998**, *624*, 1642–1646.

(31) Boyer, J. L.; Ramesh, M.; Yao, H.; Rauchfuss, T. B.; Wilson, S. R. Redox-Switched Complexation/Decomplexation of K$^+$ and Cs$^+$ by Molecular Cyanometallate Boxes. *J. Am. Chem. Soc.*, in press.

(32) Kuhlman, M. L.; Rauchfuss, T. B. Structural Chemistry of "Defect" Cyanometalate Boxes: {Cs[CpCo(CN)$_3$]$_4$[Cp*Ru]$_3$} and {M[Cp*Rh-(CN)$_3$]$_4$[Cp*Ru]$_3$} (M = NH$_4$, Cs). *J. Am. Chem. Soc.* **2003**, *125*, 10084–10092.

(33) Chaudhuri, P.; Wieghardt, K. The Chemistry of 1,4,7-Triazacyclononane and Related Tridentate Macrocyclic Compounds. *Prog. Inorg. Chem.* **1987**, *35*, 329–436.

(34) Trofimenko, S. Recent Advances in Poly(pyrazolyl)borate (Scorpionate) Chemistry. *Chem. Rev.* **1993**, *93*, 943–980.

(35) Boyer, J. L.; Yao, H.; Rauchfuss, T. B.; Wilson, S. R. Cyanometallate Cages with Exchangeable Terminal Ligands/Vertices. Submitted for publication, 2006.

(36) Kuhlman, M. L. The Design of Cyanometallate Cages for Alkali Ion Separation. Ph.D. Thesis, University of Illinois-UC, Urbana, IL, 2004.

(37) (a) Haverlock, T. J.; Mirzadeh, S.; Moyer, B. A. Selectivity of Calix-[4]arene-bis(benzocrown-6) in the Complexation and Transport of Francium Ion. *J. Am. Chem. Soc.* **2003**, *125*, 1126–1127. (b) Thuery, P.; Nierlich, M.; Bryan, J. C.; Lamare, V.; Dozol, J.-F.;

Asfari, Z.; Vicens, J. Crown Ether Conformations in 1,3-Calix[4]-arene Bis(Crown Ethers): Crystal Structures of a Cesium Complex and Solvent Adducts and Molecular Dynamics Simulations. *J. Chem. Soc., Dalton Trans.* **1997**, 4191−4202. (c) Lamare, V.; Dozol, J.-F.; Fuangswasdi, S.; Arnaud-Neu, F.; Thuery, P.; Nierlich, M.; Asfari, Z.; Vicens, J. A New Calix[4]arene-bis(crown ether) Derivative Displaying an Improved Cesium over Sodium Selectivity: Molecular Dynamics and Experimental Investigation of Alkali-Metal Ion Complexation. *J. Chem. Soc., Perkin Trans. 2* **1999**, 271−284.

(38) (a) Plenio, H.; Aberle, C. Oxaferrocene Cryptands as Efficient Molecular Switches for Alkali and Alkaline Earth Metal Ions. *Organometallics* **1997**, *16*, 5950−5957. (b) Webber, P. R. A.; Beer, P. D.; Chen, G. Z.; Felix, V.; Drew, M. G. B. Bis(calix[4]diquinone) Receptors: Cesium- and Rubidium-Selective Redox-Active Ionophores. *J. Am. Chem. Soc.* **2003**, *125*, 5774−5785.

(39) Contakes, S. M.; Rauchfuss, T. B. Alkali Metal-Templated Assembly of the Tetrahedral Cyanometallate Cages [M⊂Mo$_4$(μ-CN)$_6$-(CO)$_{12}$]$^{5-}$ (M = Li, Na). *Chem. Commun.* **2001**, 553−554.

(40) Contakes, S. M.; Rauchfuss, T. B. {K[Mo$_6$(μ-CN)$_9$(CO)$_{18}$]}$^{8-}$: a Trigonal-Prismatic Cyanometalate Cage. *Angew. Chem., Int. Ed.* **2000**, *39*, 1984−1986.

(41) Yao, H. University of Illinois-UC, Urbana, IL. Unpublished work, 2004.

(42) Hamilton, B. H.; Ziegler, C. J. The Structures of Cu(I) and Ag(I) Coordination Polymers Using the Tricyanofluoroborate Anion. *Chem. Commun.* **2002**, 842−843.

(43) Kuhlman, M. L.; Yao, H.; Rauchfuss, T. B. Synthesis and Characterization of the Hexagonal Prismatic Cage {THF⊂[PhB(CN)$_3$]$_6$-[Cp*Rh]$_6$}$^{6+}$. *Chem. Commun.* **2004**, 1370−1371.

AR050215J